Journal of Materials Chemistry A

Accepted Manuscript

ROYAL SOCIETY OF CHEMISTRY

www.rsc.org/materialsA

Journal Name

RSCPublishing

COMMUNICATION

Efficient non-fullerene polymer solar cells enabled by tetrahedron-shaped core based 3D-structure small-molecular electron acceptors

Cite this: DOI: 10.1039/x0xx00000x

Received 00th January 2012,
Accepted 00th January 2012

DOI: 10.1039/x0xx00000x

www.rsc.org/

Yuhang Liu, ‡[abc] Joshua Yuk Lin Lai,‡[b] and Shangshang Chen,‡[b] Yunke Li [b], Kui Jiang [ab], Jingbo Zhao [b], Zhengke Li [b], Huawei Hu [bc], Tingxuan Ma [bc], Haoran Lin [b], Jing Liu[b], Jie Zhang[d], Fei Huang[d], Demei Yu [c] and He Yan [*ab]

Here we report a series of tetraphenyl carbon-group (tetraphenylmethane (TPC), tetraphenylsilane (TPSi) and tetraphenylgermane (TPGe)) core based 3D-structure non-fullerene electron acceptors, enabling efficient polymer solar cells with power conversion efficiency (PCE) up to ~4.3%. The results show that the TPC and TPSi core-based PSCs perform significantly better than that based on TPGe. Our study provides a new approach to design small molecular acceptor materials for polymer solar cells.

Low cost polymer solar cells (PSCs) that convert solar energy into electricity have attracted intense research interests in the past two decades[1-6]. The power conversion efficiencies (PCE) of PSCs have greatly improved from 2~3% to 10.8%[6-9] recently. Research results have shown that fullerene derivatives are most successful electron accepting materials for PSCs due to their high electron mobility, isotropic charge transport property and ability to form ideal phase separation when blended with polymers. However, fullerenes exhibit several drawbacks. The light absorption property of fullerenes is relatively weak. The complicated and costly procedures to synthesize and purify fullerene derivatives defeat the initial goal of polymer solar cells to harvest light inexpensively. These limitations drove researchers to develop non-fullerene acceptors [10-14], which has pushed the PCE of non-fullerene PSCs over 6% recently[11, 15-19]. Among the highest-performing small molecules (SMs), the perylenediimine (PDI) building block is widely used to construct inexpensive electron acceptors for PSCs [16, 17, 20-22]. The strong electron withdrawing dicarboximide groups on PDI make it an excellent electron accepting material with electron mobility on the order up to 10^1 cm^2 V^{-1} s^{-1} [23]. PDI derivatives can be produced in large quantities and are much easier to purify compared with fullerenes[24, 25]. Their energy levels can also be easily tuned by structural modifications. However, unlike ball-shaped fullerenes, PDI based SMs tend to form strong aggregates due to their large near-planar structures, leading to large domains in donor-acceptor blends that are detrimental to PSC performances. Reducing the self-aggregation tendency of PDI based SMs should be taken under consideration in designing novel SM acceptor structures. Previous work to modify PDI generally followed this strategy: two PDI units are linked together using bulky or twisted groups such as thiophene[21, 23], benzene, biphenyl[26], or spiro-fluorine[11, 27]. This strategy decreases the aggregation between PDI based molecules, but the electron mobilities of the SM acceptors are also reduced.

3D-structure SM acceptors are one of the most promising approaches to obtain high mobility yet relatively small feature sizes for PSCs. These SMs may form readily interconnecting charge transport networks that exhibit sufficient electron mobility. Also, a 3D core may decrease the crystallinity of the PDI based SMs, thus preventing the formation of excessively large domains in PSCs. In 2014, Zhan and coworkers reported a quasi-3D SM acceptor that enabled non-fullerene PSCs with a high PCE up to 3.4% [28]. We also reported a tetraphenylethylene core based 3D SM acceptor that could form amorphous films with relatively small feature sizes yet still exhibit reasonably high electron mobility. As a result, a high PCE of 5.5% was achieved based on this SM acceptor[26].

To get more insights in the design and application of 3D SM acceptors, here we report a series of 3D-structure SM acceptors based on tetrahedron-shaped cores connected with four PDI units. These SM materials have similar 3D structures except that the sizes of the core atoms (C, Si, Ge) are different. The structures and synthesis of the SM acceptors are shown in Scheme 1. The SM acceptors can be synthesized via Suzuki cross coupling reactions. All SM acceptors show two sharp doublets in the aromatic region in the ^{1}H NMR spectra that

correspond to the two pairs of protons on the benzene ring. This indicates that the phenyl group attached to the core atom can freely rotate in solution. The other peaks in the aromatic region can be clearly assigned to the protons on PDI. The electrical-chemical properties of the SM acceptors were characterized by cyclic voltammetry (Fig. 1a). The HOMO and LUMO levels of the three SMs (summarized in table 1) are comparable. The LUMO levels of the SMs should provide sufficient LUMO offset for excitons dissociation when the SMs are blended with common low-band-gap polymers.

The UV-Vis absorption spectra of the SM acceptors (Fig. 1b) show that the absorption onsets of these SM acceptors are almost identical, which indicates that the optical bandgaps of these SM acceptors are similar. Compared to PDI monomer, the partial conjugation between the phenyl group and PDI group made the optical onset of TPC-PDI_4, TPSi-PDI_4 and TPGe-PDI_4 extend from 550 nm to ~595 nm. Note that the optical bandgaps of the SM acceptors are estimated to be about 2.2 eV, which is complementary to that of the state-of-art low bandgap polymers. The electron mobilities of TPC-PDI_4, TPSi-PDI_4 and TPGe-PDI_4 were characterized by space charge limit charge (SCLC) method with device structures of ITO/ZnO/SM acceptor/Ca/Al. The electron mobilities of the SMs were summarized in table 1.

To further explore the potential applications of these SMs as electron acceptors in PSCs, we fabricated solar cell devices with a commonly used low bandgap donor polymer (PffBT4T-2DT[29]) with a device structure of ITO/ZnO/Polymer:SM acceptor/V_2O_5/Al. All the devices were capsulated in a glove box and measured in ambient conditions under 100 mW cm^{-2} AM 1.5G simulated solar illumination. The PSC performances of these non-fullerene based PSC devices are summarized in table 1. A PCE of 4.3%, an outstanding open circuit voltage (V_{OC}) of 0.96 eV, a short circuit current (J_{SC}) of 9.2 mA cm^{-2}, and a fill factor of 49% were achieved for TPC-PDI_4 based PSC devices. Typical *J-V* plots of the SM acceptors based PSCs is shown in Fig. 1c. For the donor polymer PffBT4T-2DT, the UV-Vis absorption onset and peak are estimated at 760 nm and 700 nm, whereas its absorption is much weaker in the short wavelength range, where the absorption of the SMs is relatively strong. The absorption spectra of the SMs, donor polymer and blend films are shown in figure 2b and figure S1, indicating that the light absorption property of PffBT4T-2DT is much weaker than the SMs in 450 – 550 nm range, whereas the EQE value in 450 – 550 nm is similar or higher than that in 600 – 750 nm range. The results reveal that the SM acceptors do contribute to the photocurrent in the short wavelength range (450 – 550 nm). Note that the device fabrication processes do not involve any solvent additives or interlayers, indicating that these SM acceptors could be easily applied to fast and roll-to-roll industrial processing.

In order to get more insights into the morphology of the SM acceptors based PSCs, we first carried out X-ray diffraction (XRD) experiments of the neat SM films and blend films. The TPC-PDI_4, TPSi-PDI_4 and TPGe-PDI_4 neat and blend films are shown to be completely amorphous (Figure 2a, Figure S2). It is commonly known that PDI tended to aggregate and form large crystal domains because of its large near-planar structure. PDI based SM acceptors must introduce bulky or twisted groups to prevent the strong crystallization. The UV-Vis absorption spectra of the films cast by the SMs are shown in Fig. 2b. Compared to the UV-Vis absorption spectra of the solutions, the optical onsets of the films are slightly red-shifted around 30 nm, which is much smaller than that for PDI monomer (the red-shift is around ~100 nm). We also note that the relative intensity of the 0-1 transition peak of the film increases from the solution to the film. The increasing of 0-1 transition peak intensity and red-shift of the absorption onset from solution to film could both be related a slightly stronger extent of molecular aggregation of the SM in the film than in solution (Detailed discussion and supporting data were shown in ESI figure S3). Due to the bulky tetrahedron shaped cores of the SM acceptors, the aggregation tendency of the PDI unit is effectively reduced as supported by XRD data, indicating that the tetrahedron-core based SMs are suitable candidates as PSC acceptors. The blend morphology of these SM acceptors based PSCs were then characterized by atomic force microscopy (AFM). The height and phase images are shown in Fig. 2c, 2d and 2e. The blend films show smooth surfaces with feature sizes around 20-30 nm. It is known that relatively small domain size is important for efficient exciton diffusion and charge separation.

To understand the performance difference of the SMs based PSCs, light intensity dependent J_{SC} experiments were carried out (Fig. 3a). The relationship between J_{SC} and light intensity can be described by $J_{SC} = kP^S$ [17, 30]. If all free carriers are collected at the electrodes prior to recombination, S should be equal to 1 and S value of <1 indicates some extent of bimolecular recombination. The calculated *S* values for PffBT4T-2DT/TPC-PDI_4, PffBT4T-2DT/TPSi-PDI_4, and PffBT4T-2DT/TPGe-PDI_4 are 0.96, 0.97 and 0.92 respectively. The results show that the bimolecular recombination is relatively weak for PffBT4T-2DT/TPC-PDI_4 and PffBT4T-2DT/TPSi-PDI_4 films, but slightly stronger for PffBT4T-2DT/TPGe-PDI_4 film. Light intensity dependence of the V_{OC} of the SM-based PSCs were also characterized. The results are shown in Fig. 3b, with the lines being the fits following the relationship of "$V_{OC} = \alpha kBT/q \ln P$ + constant". The calculated α for PffBT4T-2DT/TPC-PDI_4, PffBT4T-2DT/TPSi-PDI_4, and PffBT4T-2DT/TPGe-PDI_4 are 1.12, 1.20 and 1.78 respectively, which indicates stronger monomolecular recombination at the open circuit condition in PffBT4T-2DT/TPGe-PDI_4 film. Lastly, photocurrent density versus effective voltage characterization was carried out. Photocurrent density (J_{ph}, defined as J_L - J_D, where J_L and J_D are the current densities under illumination and in the dark, respectively) as a function of effective voltage (V_{eff}, defined as V_0 - V, where V_0 is the voltage at which J_{ph} is zero) was shown in Fig. 3c following

procedures in previous reports [31 32 33]. The calculated charge dissociation probabilities $P(E,T)$ are 78%, 83% and 63% for the devices of PffBT4T-2DT/TPC-PDI$_4$, PffBT4T-2DT/TPSi-PDI$_4$ and PffBT4T-2DT/TPGe-PDI$_4$, respectively. This could be one of the issues that caused the lower EQE of PffBT4T-2DT/TPGe-PDI$_4$ based PSCs[34, 35]. All these results combined, could explain why PffBT4T-2DT/TPC-PDI$_4$ and PffBT4T-2DT/TPSi-PDI$_4$ perform better than PffBT4T-2DT/TPGe-PDI$_4$ based PSCs.

In summary, a family of tetrahedron core-based 3D-structure SM acceptors are synthesized and characterized. PSC devices were fabricated achieving PCE up to 4.3% and an outstanding V_{OC} of 0.96 V, which is much higher than that *V*oc of the corresponding polymer/fullerene devices. To understand why TPC-PDI$_4$ and TPGe-PDI$_4$ based PSCs perform better than that based on TPGe-PDI$_4$, XRD, AFM, light intensity dependence of the J_{SC} and V_{OC}, and photocurrent density versus effective voltage experiments are carried out. The results of XRD and AFM measurements show that all these three SMs can form smooth films and relatively small feature sizes when blended with PffBT4T-2DT. The calculated exciton germinate recombination and bimolecular recombination results show that bimolecular recombination of PffBT4T-2DT/TPC-PDI$_4$ and PffBT4T-2DT/TPSi-PDI$_4$ is weaker than that of PffBT4T-2DT/TPGe-PDI$_4$. These reasons combined provided a reasonable explanation why PffBT4T-2DT/TPC-PDI$_4$ and PffBT4T-2DT/TPSi-PDI$_4$ perform better than PffBT4T-2DT/TPGe-PDI$_4$. This work provides a new design strategy for 3D structure electron acceptors enabling efficient non-fullerene PSCs.

Notes and references

[a]*Hong Kong University of Science and Technology-Shenzhen Research Institute, No. 9 Yuexing 1st RD, Hi-tech Park, Nanshan, Shenzhen 518057, China. E-mail: hyan@ust.hk*

[b]*Department of Chemistry, The Hong Kong University of Science and Technology, Clear Water Bay, Hong Kong.*

[c]*Joint School of Sustainable Development and MOE Key Lab for Non-Equilibrium Synthesis and Modulation of Condensed Matter, Xi'an Jiaotong University, Xi'an 710049, P R China.*

[d]*Institute of Optoelectronic Materials and Devices, State Key Laboratory of Luminescent Materials and Devices, South China University of Technology, Guangzhou, 510640, P.R.China.*

† Electronic supplementary information (ESI) available: Materials and methods, See DOI:

‡ These authors contributed equally.

Acknowledgements

The work described in this paper was partially supported by the National Basic Research Program of China (973 Program; 2013CB834701), the Hong Kong Innovation and Technology Commission (ITS/354/12), the Hong Kong Research Grants Council (T23-407/13 N, N_HKUST623/13, and 606012) and the National Science Foundation of China (#21374090).

1. J. Peet, J. Y. Kim, N. E. Coates, W. L. Ma, D. Moses, A. J. Heeger and G. C. Bazan, *Nature materials*, 2007, **6**, 497-500.
2. J. J. M. Halls, C. A. Walsh, N. C. Greenham, E. A. Marseglia, R. H. Friend, S. C. Moratti and A. B. Holmes, *Nature*, 1995, **376**, 498-500.
3. G. Yu, J. Gao, J. C. Hummelen, F. Wudl and A. J. Heeger, *Science*, 1995, **270**, 1789-1791.
4. G. Li, V. Shrotriya, J. Huang, Y. Yao, T. Moriarty, K. Emery and Y. Yang, *Nature materials*, 2005, **4**, 864-868.
5. H.-Y. Chen, J. Hou, S. Zhang, Y. Liang, G. Yang, Y. Yang, L. Yu, Y. Wu and G. Li, *Nat Photon*, 2009, **3**, 649-653.
6. J. You, L. Dou, K. Yoshimura, T. Kato, K. Ohya, T. Moriarty, K. Emery, C.-C. Chen, J. Gao, G. Li and Y. Yang, *Nature communications*, 2013, **4**, 1446.
7. S. H. Liao, H. J. Jhuo, P. N. Yeh, Y. S. Cheng, Y. L. Li, Y. H. Lee, S. Sharma and S. A. Chen, *Scientific reports*, 2014, **4**, 6813.
8. Y. Liu, J. Zhao, Z. Li, C. Mu, W. Ma, H. Hu, K. Jiang, H. Lin, H. Ade and H. Yan, *Nature communications*, 2014, **5**, 5293.
9. L. Zuo, C. C. Chueh, Y. X. Xu, K. S. Chen, Y. Zang, C. Z. Li, H. Chen and A. K. Jen, *Adv Mater*, 2014, **26**, 6778-6784.
10. S.-Y. Liu, C.-H. Wu, C.-Z. Li, S.-Q. Liu, K.-H. Wei, H.-Z. Chen and A. K. Y. Jen, *Advanced Science*, 2015, **2**, n/a-n/a.
11. J. Zhao, Y. Li, H. Lin, Y. Liu, K. Jiang, C. Mu, T. Ma, J. Y. Lin Lai, H. Hu, D. Yu and H. Yan, *Energy Environ. Sci.*, 2015, **8**, 520-525.
12. T. Earmme, Y. J. Hwang, N. M. Murari, S. Subramaniyan and S. A. Jenekhe, *Journal of the American Chemical Society*, 2013, **135**, 14960-14963.
13. K. Cnops, B. P. Rand, D. Cheyns, B. Verreet, M. A. Empl and P. Heremans, *Nature communications*, 2014, **5**, 3406.
14. C. Mu, P. Liu, W. Ma, K. Jiang, J. Zhao, K. Zhang, Z. Chen, Z. Wei, Y. Yi, J. Wang, S. Yang, F. Huang, A. Facchetti, H. Ade and H. Yan, *Advanced Materials*, 2014, **26**, 7224-7230.
15. A. a. F. Eftaiha, J.-P. Sun, I. G. Hill and G. C. Welch, *J. Mater. Chem. A*, 2014, **2**, 1201-1213.
16. A. Sharenko, C. M. Proctor, T. S. van der Poll, Z. B. Henson, T. Q. Nguyen and G. C. Bazan, *Adv Mater*, 2013, **25**, 4403-4406.
17. Y. Zang, C. Z. Li, C. C. Chueh, S. T. Williams, W. Jiang, Z. H. Wang, J. S. Yu and A. K. Jen, *Adv Mater*, 2014, **26**, 5708-5714.
18. Y. Lin, J. Wang, Z. G. Zhang, H. Bai, Y. Li, D. Zhu and X. Zhan, *Adv Mater*, 2015, **27**, 1170-1174.
19. Y. Lin, Z.-G. Zhang, H. Bai, J. Wang, Y. Yao, Y. Li, D. Zhu and X. Zhan, *Energy Environ. Sci.*, 2015, **8**, 610-616.
20. X. Zhang, C. Zhan and J. Yao, *Chemistry of Materials*, 2015, **27**, 166-173.
21. Z. Lu, B. Jiang, X. Zhang, A. Tang, L. Chen, C. Zhan and J. Yao, *Chemistry of Materials*, 2014, **26**, 2907-2914.
22. A. Sharenko, D. Gehrig, F. Laquai and T.-Q. Nguyen, *Chemistry of Materials*, 2014, **26**, 4109-4118.
23. X. Zhang, Z. Lu, L. Ye, C. Zhan, J. Hou, S. Zhang, B. Jiang, Y. Zhao, J. Huang, S. Zhang, Y. Liu, Q. Shi, Y. Liu and J. Yao, *Adv Mater*, 2013, **25**, 5791-5797.
24. X. Zhan, A. Facchetti, S. Barlow, T. J. Marks, M. A. Ratner, M. R. Wasielewski and S. R. Marder, *Adv Mater*, 2011, **23**, 268-284.
25. C. Huang, S. Barlow and S. R. Marder, *The Journal of organic chemistry*, 2011, **76**, 2386-2407.
26. Y. Liu, C. Mu, K. Jiang, J. Zhao, Y. Li, L. Zhang, Z. Li, J. Y. Lai, H. Hu, T. Ma, R. Hu, D. Yu, X. Huang, B. Z. Tang and H. Yan, *Adv Mater*, 2015, **27**, 1015-1020.
27. Q. Yan, Y. Zhou, Y.-Q. Zheng, J. Pei and D. Zhao, *Chemical Science*, 2013, **4**, 4389.
28. Y. Lin, Y. Wang, J. Wang, J. Hou, Y. Li, D. Zhu and X. Zhan, *Adv Mater*, 2014, **26**, 5137-5142.
29. Z. Chen, P. Cai, J. Chen, X. Liu, L. Zhang, L. Lan, J. Peng, Y. Ma and Y. Cao, *Adv Mater*, 2014, **26**, 2586-2591.
30. L. Lu, T. Xu, W. Chen, E. S. Landry and L. Yu, *Nature Photonics*, 2014, **8**, 716-722.
31. L. Ye, W. Jiang, W. Zhao, S. Zhang, D. Qian, Z. Wang and J. Hou, *Small*, 2014, **10**, 4658-4663.
32. V. D. Mihailetchi, L. J. A. Koster, P. W. M. Blom, C. Melzer, B. de Boer, J. K. J. van Duren and R. A. J. Janssen, *Advanced Functional Materials*, 2005, **15**, 795-801.

33. Z. Li, J. D. A. Lin, H. Phan, A. Sharenko, C. M. Proctor, P. Zalar, Z. Chen, A. Facchetti and T.-Q. Nguyen, *Advanced Functional Materials*, 2014, **24**, 6989-6998.
34. C. M. Proctor, S. Albrecht, M. Kuik, D. Neher and T.-Q. Nguyen, *Advanced Energy Materials*, 2014, **4**, n/a-n/a.
35. A. J. Heeger, *Adv Mater*, 2014, **26**, 10-27.

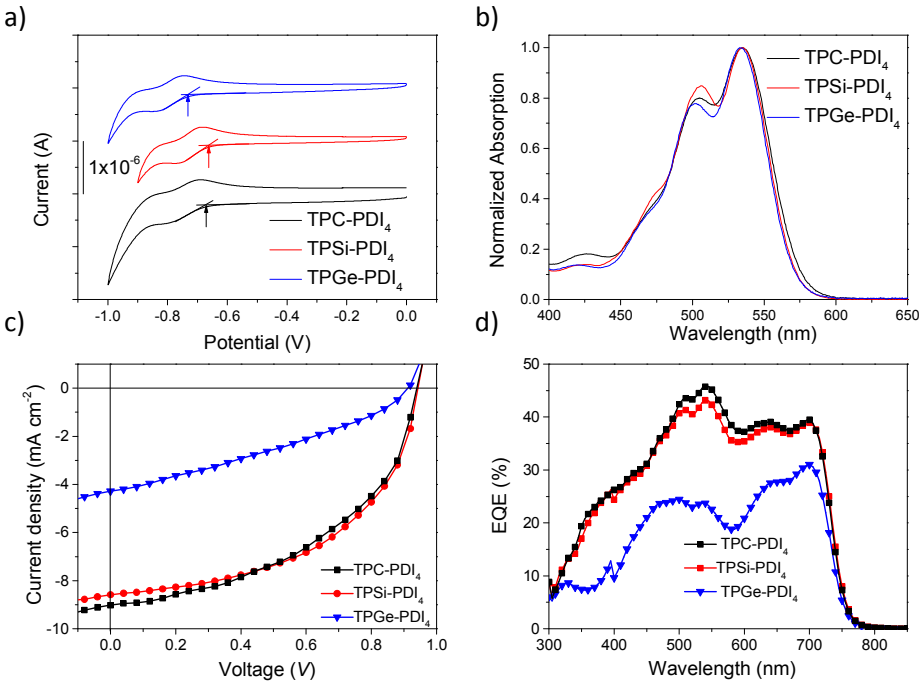

Figure 1 a) Cyclic voltammetry results of the SM acceptors. **b)** Normalized UV-Vis absorption spectra of the SM acceptors in chloroform solutions. **c)** *J-V* characteristics of PffBT4T-2DT/TPC-PDI$_4$, PffBT4T-2DT/TPSi-PDI$_4$ and PffBT4T-2DT/TPGe-PDI$_4$ devices. **d)** EQE spectra of the devices.

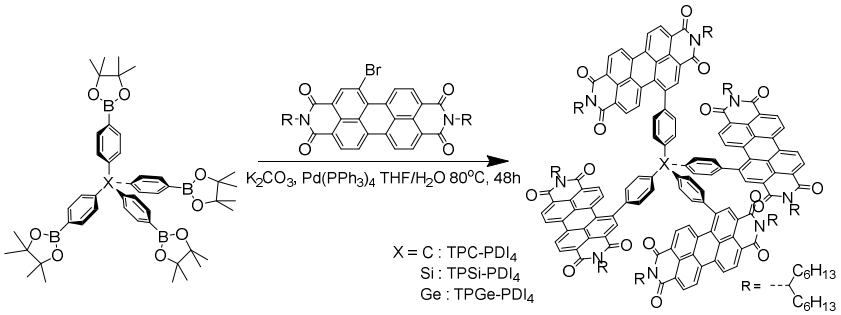

Scheme 1. Synthetic procedures of TPC-PDI_4, TPSi-PDI_4 and TPGe-PDI_4.

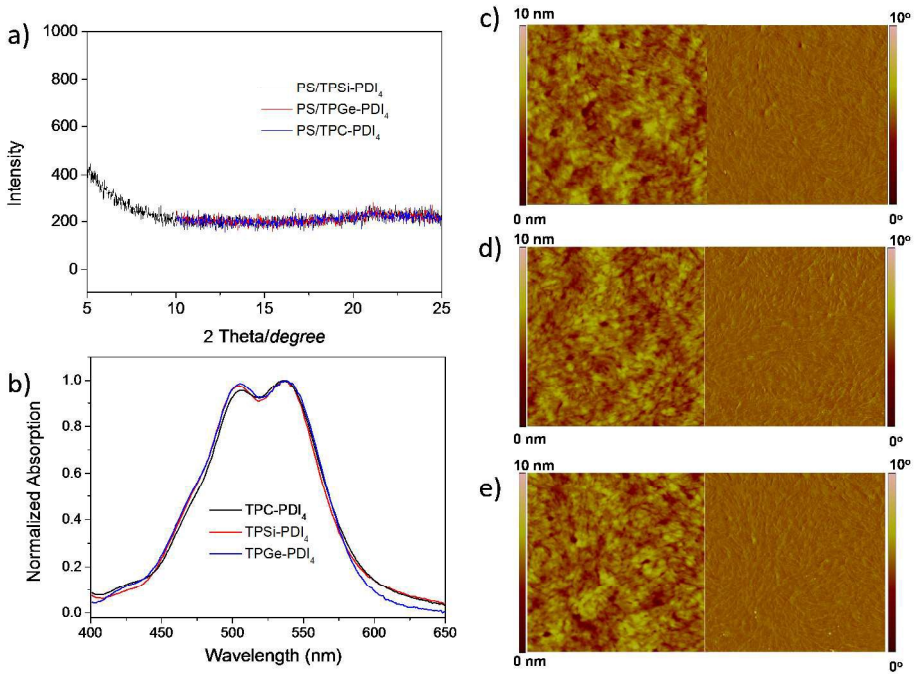

Figure 2 a) X-ray diffraction (XRD) pattern of TPC-PDI$_4$, TPSi-PDI$_4$, and TPGe-PDI$_4$ films. **b)** Normalized UV-Vis absorption of the SMs as films. AFM images (1 × 1 μm) of the BHJ films casted with: **c)** PffBT4T-2DT:TPC-PDI$_4$, **d)** PffBT4T-2DT:TPSi-PDI$_4$, **e)** PffBT4T-2DT:TPGe-PDI$_4$.

Table 1. Characterization data of the SMs and PSC performances of the SMs based PSCs. [a] cal. by opt. bandgap and CV. [b] measured by CV.

Active Layer	HOMO level of the SM [eV][a]	Opt. bandgap [eV]	LUMO level of the SMs [eV][b]	e-mobility [$cm^2\ V^{-1}\ s^{-1}$]	V_{OC} [V]	J_{SC} [$mA\ cm^{-2}$]	FF	PCE
PffBT4T-2DT:TPC-PDI_4	6.00	2.25	3.75	2.8×10^{-4}	0.96	9.2	0.49	4.3%
PffBT4T-2DT:TPSi-PDI_4	6.01	2.26	3.75	3.9×10^{-4}	0.94	8.5	0.53	4.2%
PffBT4T-2DT:TPGe-PDI_4	5.94	2.26	3.68	3.3×10^{-5}	0.92	5.0	0.37	1.6%

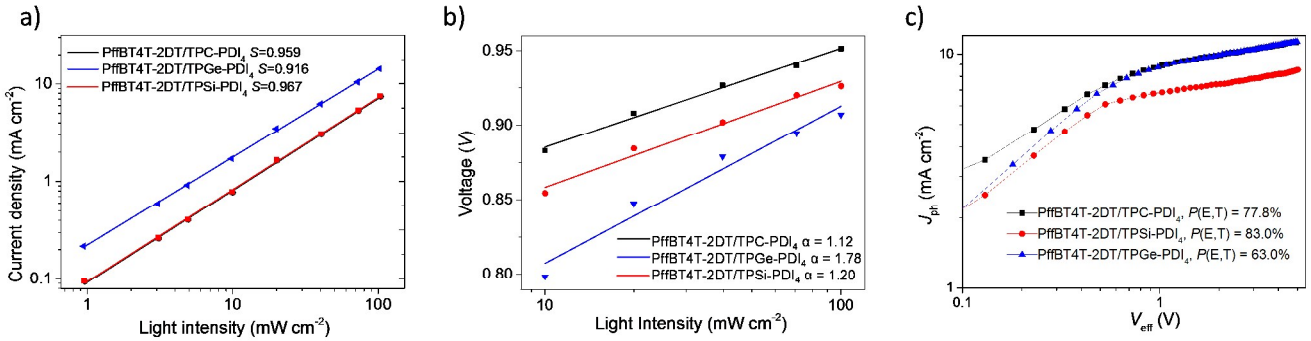

Figure 3 a) Light intensity dependence of the short circuit current of the PSC devices. **b)** Light intensity dependence of the open circuit voltage of the PSC devices. **c)** Photocurrent density versus effective voltage characteristics of the SM based PSC devices.